Earth and Planetary Science Letters, 106 (1991) 151–168
Elsevier Science Publishers B.V., Amsterdam

[XLeP]

Multi-method radiometric dating of volcano-sedimentary layers from northern Italy: age and duration of the Priabonian stage

G.S. Odin [a], V. Barbin [b], A.J. Hurford [c], H. Baadsgaard [d], B. Galbrun [e] and P.-Y. Gillot [f]

[a] *Géochronologie et Sédimentologie Océanique, Université P. and M. Curie, 4 Place Jussieu, F75252 Paris, France*
[b] *Geologisches Institut, Universität Bern, CH 3012 Berne, and Muséum d'Histoire Naturelle, 1 Route de Malagou, C.P. 434, CH 1211 Genève 6, Switzerland*
[c] *Department of Geological Sciences, University and Birkbeck Colleges, Gower Street, London WC1E 6BT, UK*
[d] *Department of Geology, 158 Earth Science Bldg, University of Alberta, Edmonton, Alta. T6G2E3, Canada*
[e] *Stratigraphie, Unité Tectonique et Stratigraphie CNRS, Université P. and M. Curie, 4 Place Jussieu, F75252 Paris, France*
[f] *CEA–CNRS, UG Centre des faibles radioactivités, Bat 444, 91191 Gif-sur-Yvette, France*

Received March 5, 1991; revised and accepted June 26, 1991

ABSTRACT

A comparison between conventional K–Ar (biotite) ages and fission track (zircon and apatite) and U–Pb (zircon) ages obtained from stratigraphically well-constrained Priabonian (Late Eocene) volcano-sedimentary deposits of northern Italy is presented. Two sections at Priabona (one level) and Possagno (two levels) were dated. The application of fission track dating appears fruitful for obtaining reasonably precise (± 4 to 5% 2σ errors) ages useful for time-scale calibration. The concordancy of apatite and zircon fission track ages, and the reproducibility of results provide the time of volcanic eruption and deposition. The U–Pb analysis of the zircons has not been unsuccessful, but discordancy does not permit accurate dating. Significant dates obtained from Possagno are: K–Ar method, 35.0 ± 0.5 Ma (duplicate analysis on K-rich biotite from the same level); fission track dating method, 35.8 ± 1.4 Ma (weighted mean age on 2 apatite and 3 zircon separates from the same level); U–Pb method, 36.7 ± 1.0 Ma (maximum age of discordant zircons from the same level). The comparison between the present results and recent multi-method and multi-laboratory results obtained from time equivalent Priabonian (Late Eocene) biotite-rich layers from the Apennines shows perfect agreement and supports the location of a Priabonian stage between about 37.5 Ma and about 33.7 (± 0.5) Ma; the alternative ages preferred by the Decade of North American Geology convention should be abandoned and a large portion of this scale revised accordingly.

1. Introduction

The numerical age of the Eocene–Oligocene boundary is a much-debated question which is part of a more general problem of time-scale calibration. Against the old estimate of 37–38 Ma suggested in 1964, an estimate some 10% younger was subsequently concluded [1]. Despite this, an estimate of ~ 37 Ma is still used by a number of workers who follow the convention proposed by Palmer [2] using the results of a long-term "magnetic extrapolation" between doubtful tie points [3, 4, 5]. The major reason usually quoted for selection of the old age is that the estimate of 34 Ma was derived from the dating of glaucony [1], the results being suspected of providing apparent ages which were "too young". This argument of a systematic lowering of glaucony ages (as well as ages from other geochronometers consistent with glaucony ages) results in age estimates for the whole of the Palaeogene and other portions of this conventional time scale [2] which are much older than might be concluded from combining results of selected glaucony and other geochronometer analyses. In order to resolve this dispute, a search has been undertaken for new (non-glaucony) samples which, from geological arguments, should provide reliable radiometric ages. A number of such samples were found in Late Eocene and Oligocene deposits. Several of the best possibilities of calibrating the numerical age of the Priabonian sediments, are located in Italy (Fig. 1).

A first set of radiometric dates from the Apennines [6] was recently supplemented, reinterpreted

0012-821X/91/$03.50

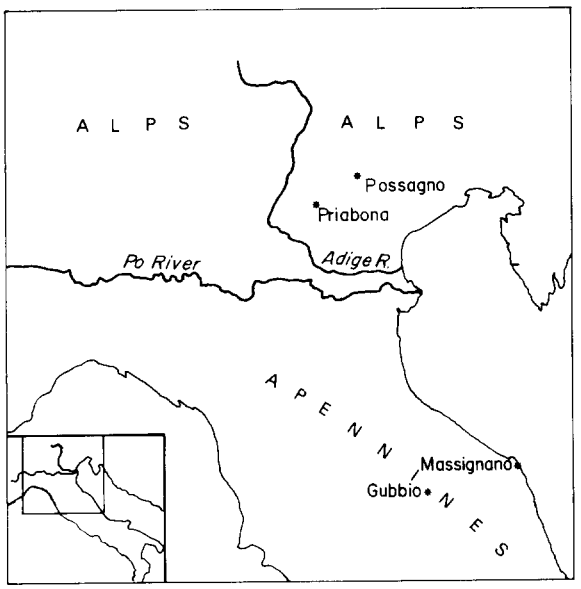

Fig. 1. Location of radiometrically dated Late Eocene samples in the Apennines (Massignano and Gubbio) and northern Italy (Priabona and Possagno).

and summarized in the light of further results in both the geochronological and stratigraphical domains [7]. A second area was prospected near Priabona where the biostratigraphy of long-known sections has been revised [8]. A biotite extracted from a nearly basal Priabonian layer proved inappropriate for dating due to vermiculitisation, but small amounts of zircon and apatite were found. A preliminary study using the fission track (FT) dating method gave promising results. Finally, a third possibility was investigated around Possagno, an area submitted to a detailed biostratigraphical study during the early 1970's [9]. Four biotite-bearing layers were reported there. A geochronological investigation of these layers near Possagno began independently in three different laboratories: in Berne (V. Barbin and R. Herb), Paris (M. Zelvelder and G.S. Odin) and Zürich (H. Fischer and H. Oberhänsli).

In summary, Late Eocene material suitable for radiometric dating was identified in northern Italy at localities where the biostratigraphic constraints are fairly well established. Accordingly, an analytical program with three main aims was organised: (1) to compare the improved FT dating method and the potential of U–Pb dating for young rocks with more usual (K–Ar for calibration of these ages) dating methods; (2) to obtain new radiometric ages able to support data from the Apennines; (3) to bring data able to resolve the cited debate [3, 4, 5] concerning the actual location and duration of the Late Eocene time and therefore, indirectly to test the validity of ages deduced from reliable glauconies in Palaeogene time.

2. Analytical techniques

The magnetostratigraphic measurements were performed in Paris (by BG) using a three-axes cryogenic magnetometer (RS-01 LETI/CEA). Most of the samples were demagnetized by mixed treatment (thermal demagnetization at 150 or 200°C followed by alternating field demagnetization) which is adequate for sedimentary rocks, especially marly facies [10]. This treatment was very effective to isolate the characteristic remanent magnetization (ChRM): above 20 mT the ChRM direction was clearly defined. Detailed analytical results and discussion will be published in a companion stratigraphical paper. However, it should be emphasized that the palaeomagnetic record is well preserved and readily identified in Possagno.

A detailed description of the improved cathodoluminescence-microscope used in Berne and the corresponding analytical procedure was given previously [11]. In this study, the applied beam current density for the instrument was 0.3–0.5 $\mu A/mm^2$ at 30 keV electron energy. Luminescence characteristics were recorded on Ectachrome 400 colour slide film (developed at 800 ASA) with exposure time ranging from 2 to 8 s. The luminescence spectra were recorded on a P.T.I. series 001 monochromator equipped with a R928 Hamamatsu photomultiplier. The measured spectra were set for ± 5 nm resolution and corrected for the spectral response of the recording system between 370 and 860 nm. The luminescence was studied on polished thin sections of zircon and apatite grain mounts.

The dated biotite was prepared using magnetic separation, crushed in an agate mortar to remove possible altered layers, and cleaned ultrasonically. The conventional K–Ar technique was used because the quality of the geochronometer was good enough (K-rich, homogeneous, no trace of

vermiculite) to avoid searching for possible weathering; in addition the geochemical history of the section was known to be free of tectonometamorphic events. Potassium was measured using both atomic absorption and flame photometric techniques in Gif-sur-Yvette, using a calibration based on "Glauconite GL-O" [12]. Argon content was also measured in Gif, using the unspiked Cassignol's technique [13], the system being calibrated against reference material "Glauconite GL-O" using the interlaboratory mean of Odin and coll. [12].

Zircon and apatite were separated from 5 to 10 kg size samples; slightly more than 1.5 g of zircon were separated from a 15 kg sample collected from layer B9 in Possagno. Rough zircon separates were obtained using the conventional technique for bentonites: disaggregation and sedimentation in water, magnetic separation, bromoform and diiodomethane sedimentation, heating at 60°C in 6N nitric acid, and ultrasonic cleaning [14].

Fission track ages were measured in London using the external detector method approach [15]. ^{238}U spontaneous fission tracks were etched in the polished apatite crystals using 5N HNO_3 at 20°C for 20 s and in zircon crystals using a eutectic of KOH–NaOH at 220°C for 15 h. ^{235}U induced fission tracks were recorded in external detectors of low-uranium mica, held against the mineral mounts during irradiation with thermal neutrons, the induced tracks being subsequently etched using HF at 20°C for 45 min.

Three reactors were used during the course of this study, the changes being necessitated by the closure and non-availability of the thermal neutron irradiation facilities at Aldermaston and Harwell. The J1 thermal neutron facility of the HERALD reactor, Aldermaston, UK, was described in Hurford and Green [16]; the thermal column of the PLUTO reactor, Harwell, UK, has a Cd ratio for gold > 300, whilst the X7 thermal position in the HIFAR reactor, Lucas Heights, NSW, Australia, has a Cd ratio of > 200 for gold. Track counting utilised ZEISS Axioplan® microscopes with a total magnification of $1250\times$, apatite being counted with a $100\times$ dry objective and zircon with a $100\times$ oil objective. The microscopes were equipped with Stagemover computerised stage systems to locate the zircon crystals and their mirror image mica impressions. Neutron fluxes were monitored by including wafers of uranium dosimeter glasses SRM612, CN1 [16] or CN5 (Corning® glass with about 11 ppm natural uranium) at either end of the sample stack, and counting the induced tracks recorded in a mica detector held against the glass. In addition, horizontal confined spontaneous track length distributions were measured for each apatite sample using a microscope equipped with a drawing tube and digitising tablet. Only well-etched prismatic sections of apatite and zircon were selected for length and age measurement, identified by the alignment of etch pits under reflected light. Sample ages (Table 3) were calculated using the zeta (ζ) calibration approach using ζ-values determined by repeated analysis of age standards [16]. The reactor and dosimeter glass used for each analysis is shown in Table 3 together with the appropriate value for ζ. As a control of calibration, aliquots of zircon and apatite age standards were included in each irradiation and the analytical results are also shown in Table 3. Analyses were subjected to a χ^2-test [17] to determine whether extra-Poissonian error might be present. Each data set passed the test at $> 5\%$ level, indicating the Poissonian error shown (the conventional error of Green [18]) derived from counting statistics to be a reasonable estimator of experimental error.

U–Pb ages were obtained using the conventional multi-grain technique in Edmonton [19].

3. Stratigraphical setting

Munier-Chalmas and de Lapparent [20] first proposed the Priabonian stage: "Du nom de Priabona, dans les Colli Berici, nous tirerons le nom de Priabonien." Hardenbol [21] suggested that the section at Priabona, although not in the Colli Berici but in the Monte Lessini (Fig. 2), should be designated as the type section of the stage. At the Eocene colloquium [22], a general agreement was obtained and it was decided that the section in Priabona be taken as the stratotype. Five para-stratotypes were also defined (see Fig. 2): (1) Granella section, (2) Ghenderle section (= Bressana), (3) Brendola section, (4) Mossano section, and (5) Possagno section [22].

The comparative stratigraphy of the sections quoted in this paper is shown in Fig. 3. The stratigraphy of the sections in the Lessini and

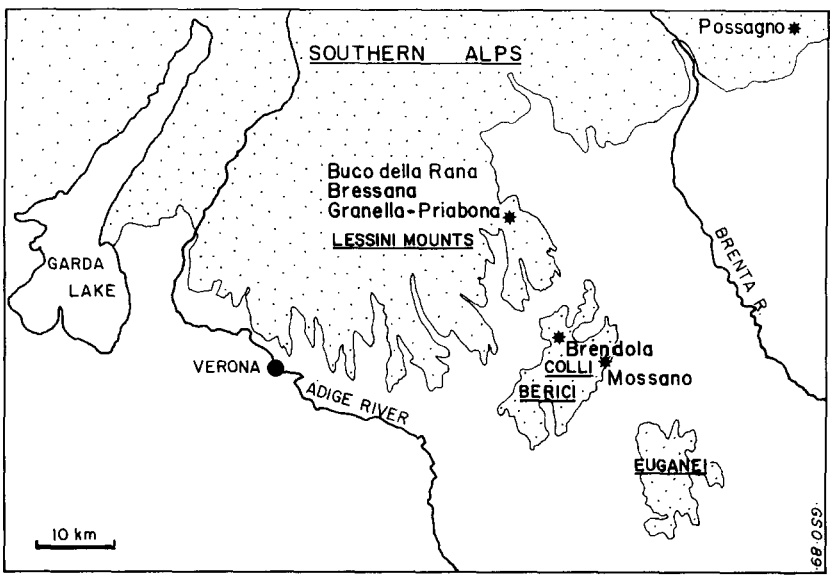

Fig. 2. Detailed map of the Priabonian sections quoted in the text. A single star is shown for the very near 4 localities in the Priabona area. The dotted area indicates Meso and Cenozoic formations as opposed to Quaternary alluvium.

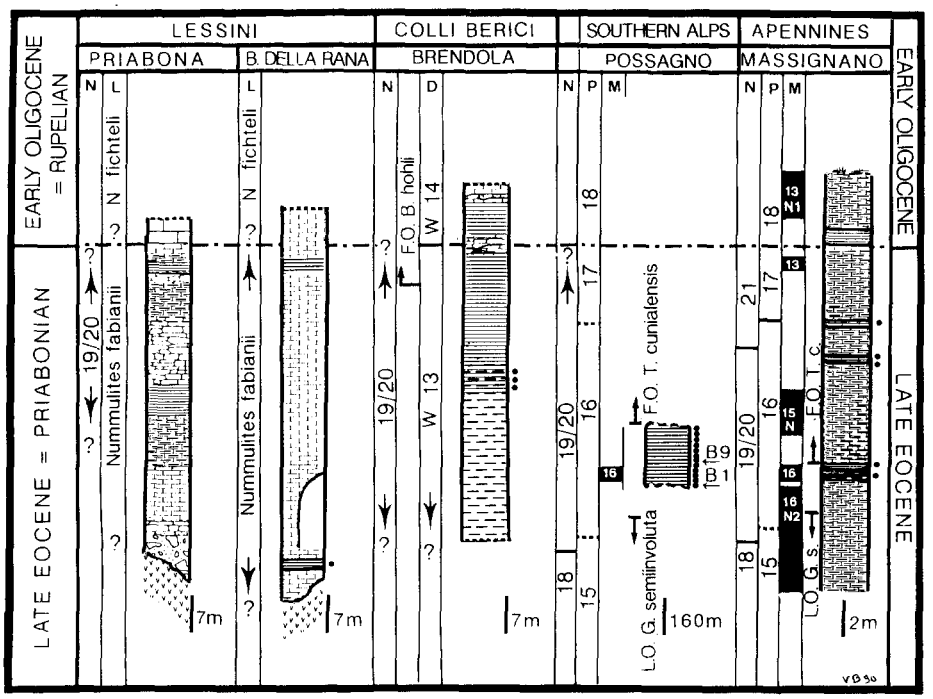

Fig. 3. Comparative stratigraphical location of the sections quoted (V. Barbin, unpublished). Note that the scale thickness shown at the bottom of each column is dissimilar for the different sections, but the time is approximately of a similar scale for all sections. *D* = Dinoflagellate zonation; *L* = larger foraminifer zonation; *M* = magnetostratigraphic control; *N* = calcareous nannofossil zonation; *P* = planktonic foraminifer zonation; black dots indicate volcano-sedimentary deposits

Berici is documented with fossils. Calcareous nannoplankton is present in portions of the Priabona, Bressana and Brendola sections [8]. The larger foraminifer *Nummulites fabianii* occurs locally in the Priabona, Granella, and Buco della Rana sections as well as near Possagno. The Dinoflagellate biozone W 13 is present in portions of the Bressana and Brendola sections [23]. The end of Eocene time is denoted by the first occurrence of Dinoflagellates *Phthanoperidium amoenum*, *Wetzeliella gochtii*, and pollenites *Boehlensipollis hohli*, at the top of the Brendola section [24, 25].

In Possagno, different fossil groups were studied for biostratigraphy [9]. The most precise biostratigraphic subdivision, for the interval discussed here, was obtained from planktonic foraminifers by Toumarkine [in 9]. The section sampled for the present study is located between the last occurrence (= LO) of *Globigerinatheka semiinvoluta* and the first occurrence (= FO) of "*Globorotalia (Turborotalia) cerroazulensis cunialensis*" (= *T. cunialensis*); this indicates the early portion of the planktonic foraminiferal zone P16 of Blow. In short, the volcano-sedimentary layers sampled for radiometric dating are definitively located within the lower half of the Late Eocene Priabonian stage, but not at its base.

In Massignano (modern type locality for the Eocene–Oligocene boundary [26]), the two quoted foraminiferal events (LO *G. semiinvoluta*—FO *T. cunialensis*) are located at levels +4.5 m and +7.5 m above the base of the section, respectively (Fig. 3). In this section, the greatest number of stratigraphic tools were available including planktonic foraminifers, calcareous nannofossils, magnetostratigraphy, isotopic and elementary geochemistry, and geochronology.

This 3 m thick interval in Massignano represents a time interval of 0.4 Ma (±0.1) Ma, taking the rate of sedimentation to be 8 m (±2) per Ma [27]. The same interval corresponds to more than 200 m of clay in Possagno. If the time duration between the two events is similar in the two areas, then the sedimentation rate in Possagno can be estimated at ~ 500 m/Ma. An alternative estimate may be derived by considering the total thickness of the entire Late Eocene series in Possagno, 750 m, deposited over a time interval of 3 to 4 Ma [2, 4, 5]—a mean sedimentation rate of ~ 200 m/Ma, assuming that no portion of the series contains a break in sedimentation (no break is actually documented). However, according to Cita [in 9], the sedimentation rate is increased at the top of the series and thus, to balance the section, a reduced sedimentation rate of ~ 150 m/Ma can be suggested for the lower portion of the section studied. The first estimate uses as reference the interval of time between two biostratigraphic "events" and is thus less reliable than the second estimate based on the absence of a sedimentation break. Accordingly, the second lower sedimentation rate is to be preferred.

In order to supplement the biostratigraphic constraint, and because precise calibration of the sedimentary sequence should consider the magnetic record, we have undertaken a magnetostratigraphic study in the Possagno Quarry. The results of this study will be discussed elsewhere and are briefly quoted below. From the base of the section to the top (about 185 m, see Fig. 4), 47 levels have been sampled. Two additional levels, stratigraphically located about 50 m above this quarry section, were sampled in a small outcrop located 200 m to the south of the Bassano–Possagno road. Each level was cored twice and two distinct cores prepared for measurements. An example of demagnetization behaviour is given Fig. 5.

The fundamental results are as follows: five successive horizons have been found to show a reproducible normal polarity; all other levels indicate a reversed initial magnetization. Intermediate polarity was suspected in the uppermost sample of the section (at level 240 m above the base of the studied section). This level could correspond to the beginning of the next normal polarity zone. The normal episode defined by the 5 successive horizons covers a minimum of 20 m and a maximum of 45 m (Fig. 4). If our estimate of the sedimentation rate is realistic, this episode should represent an interval of time of between 0.1 and 0.45 Ma.

This short normal episode found in Possagno is located between LO of *semiinvoluta* and FO of *cunialensis*; the same biostratigraphic events found in the section of Massignano (Fig. 4) bracket a single short normal episode: 16N1 [26, 28]. In Massignano, episode 16N1 (1 m thick) represents about 0.15 Ma [28]; this duration is compatible with the one calculated from Possagno, and we interpret the normal episode in Possagno as 16N1.

In the Massignano section, this 16N1 episode is followed by a reversed episode (15R) which is about twice as long (twice as thick) as 16N1; if the sedimentation rate was regular in Possagno, this would correspond to about 40 to 90 m. In fact, the thickness of sediment which shows a reverse magnetic polarity above the short normal episode in Possagno is at least 140 m thick and possibly up to 200 m. If our interpretation of the magnetostratigraphic record is correct, this confirms that the sedimentation rate during deposition of the younger part of the section was much higher than that during deposition of the older part of the section.

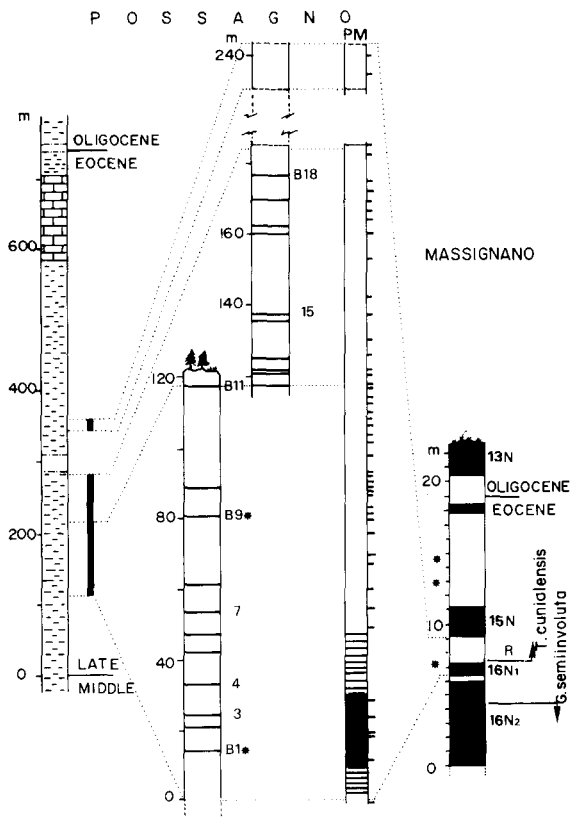

Fig. 4. Stratigraphy of the section at Possagno. Left: section of the Late Eocene series in the Possagno area; the 590 m thick lower "Marne di Possagno" formation is overlain by the 60 m thick Santa Giustina Limestone and about 15 m of upper "Marne di Possagno". The large break of visibility shown corresponds to the Bassano–Possagno road. Middle left: the studied section consists of the 120 m thick sequence of the quarry face followed by the 65 m thick sequence of the quarry floor and an additional outcrop about 50 m above in the sequence. Numbered volcaniclastic levels (B1, 3) are the easiest to recognize. *PM* = palaeomagnetic data: black when normal polarity was identified; location of the 47 double samples measured given on the right side (dashes) of this column [Galbrun, unpublished]. Comparison with the section in Massignano [26] is given. Radiometrically dated levels are starred.

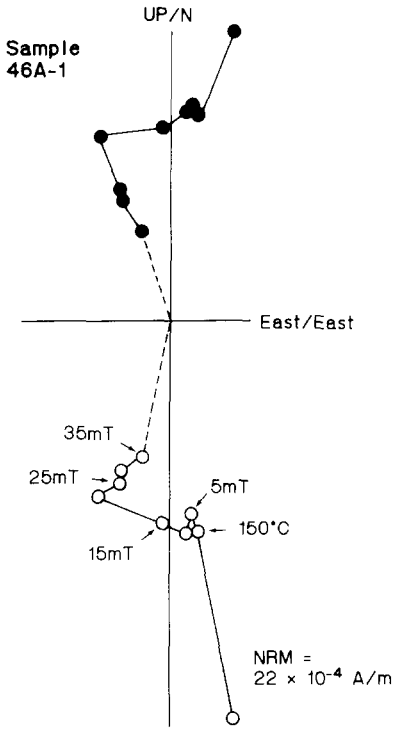

Fig. 5. Vector diagram of demagnetization of a sample at meter level 181 m. Open and solid points represent projection on the horizontal and vertical planes, respectively. The sample was heated to 150°C and progressively AF demagnetized. Above 20 mT, the ChRM is clearly defined as reversed polarity.

In summary, the volcano-sedimentary samples presently studied in northern Italy are precisely located in the Priabonian sequence (in the middle of the stage) and collected from the historical area which defined the stage. As a consequence of the combined biostratigraphic and magnetostratigraphic correlation tools, they are also accurately correlated with the section in Massignano which is already precisely dated using biotite geochronometers, which has been selected as including the new modern stratotype for the Eocene–Oligocene boundary [26]. We have, therefore, a unique opportunity to reconcile past and modern stratigraphy, to document again the numerical age of the Priabonian in a different geographical context, using different but still pyroclastic, geochronometers and different methods of dating.

4. Dated samples

4.1. Volcano-sedimentary layers

Within the Priabona area (Lessini Mounts), the Priabonian series usually begins with a volcaniclastic conglomerate. The lithologic succession defines a transgressive, followed by a regressive shallow platform sequence, that is a sedimentary cycle [8] covering the whole historical type stage. In the Priabona area, there is a single biotite-rich marly layer, ~ 1 m thick (see Fig. 3, Bucco della Rana section).

In the Colli Berici, three thin biotite-rich clay layers were observed in the Brendola section. Although there is less than 15 km between Priabona and Brendola, the biostratigraphic correlation is too poor between the coastal to neritic Lessini series and the hemipelagic Berici series to know whether or not the same volcanic event is recorded in the two localities.

In Possagno, we have studied the section located in the now disused quarry of Antonio Cunial, to the north of the Bassano–Possagno road. Here, the homogeneous middle Late Eocene "Marna di Possagno" is cut by 1 to 7 cm thick sandy layers, often harder than the rest of the formation. We have identified 11 of these layers in the quarry face. At least 9 additional layers have been recognised between the quarry face and the road, some of them being formed by 2 distinct horizons representing, however, probably less than 10,000 years between them. The time interval between the two extreme horizons (B1 and B18) is probably shorter than 0.4 Ma, and, for this reason, our geochronological study will focus mostly on a single (the most favourable) of these horizons (see Fig. 4).

X-ray diffraction from clay-size fractions collected from Late Eocene formations from the Priabona area and Brendola section indicate similar compositions, with smectite more abundant than illite, chlorite and kaolinite [8]. In the biotite-rich marl from Bucco della Rana, smectite comprises up to 95% of the clay fraction, much richer than the rest of the section, suggesting that, in this level, the clay fraction results from alteration of volcanic material. To confirm this suggestion, the clay-size fraction was separated from the biotite-rich layer and radiometrically dated using the K–Ar method. The resulting K–Ar apparent age of 85 Ma (unpublished result by M. Zelvelder and M.G. Bonhomme in Grenoble, 1987) indicates that a high proportion of the smectite in this layer is of detrital origin.

The clay-size fraction from the volcano-sedimentary layers from Possagno, is a mixture of smectite (broad peak at 15 Aå) and of a chloritized mica—or a chlorite + illite mixture—(as seen by narrow peaks at 14, 10, and 7 Aå). The clay in the rest of the series does not show a distinct difference from this composition. A similar observation was made in previous studies in the Apennines [27] and suggests common conditions of deposition in the two areas. The similar clay composition in the volcano-sedimentary layers and the rest of the series in Possagno may be explained by the high rate of (detrital) clay deposition (about 1 cm each 70 years). Speculating, if each volcano-sedimentary layer (usually 1 to 7 cm thick) results from a series of volcanic explosions over a time span of several years, then the clay resulting from the alteration of the volcanic ash should have been diluted by the rapid and constant deposition of abundant detrital clay. The polyphase nature of at least some of the volcano-sedimentary layers is well documented in the thickest layer (B9), which is clearly made of at least two distinct sandy layers separated by a 2–3 mm thick clay horizon.

Samples labelled Pos B9 (Odin), Z 208 (Barbin-Zelvelder) represent 2 different sample collections and separations from the same layer in Possagno by different authors. Sample B1 comes from a layer located 60 m below the B9 layer (Fig. 4) and is about 0.4 Ma older than B9. Sample Pos/86 (Fischer, collected by H. Oberhänsli) comes also from layer B9 as confirmed by F. Oberli (pers. commun., 1991).

4.2. Presence of geochronometers

Near Priabona, the "*marne micacée*" of Barbin [8] contains abundant biotite flakes which comprise up to 5‰ of the whole-rock, and are commonly larger than 1 to 2 mm and easily observed in hand specimens. Mainly abundant in a softer portion of the marl, about 20 to 30 cm in thickness, black biotite is widespread in the marl both above and below this soft portion, suggesting a secondary lahar-like redeposition rather than a

primary deposit following aerial transport. A biotite-rich deposit, with similar thickness and composition, has been observed to the north of Priabona in 3 different localities 1 km apart including in Bucco della Rana (M. Zelvelder, pers. commun., 1987), but is absent from the type section in Priabona. The search for other geochronometers led to separation of a small proportion of rather large apatite and zircon crystals (up to 500 μm long).

In the Brendola section of the Colli Berici, 3 biotite-bearing layers were collected during biostratigraphic investigations [8, 29]. Two of them were reinvestigated during the present study, using previously made concentrates and were found to contain less than 1‰ biotite, lower even than in the samples collected from the Priabona area. However, X-ray diffraction patterns showed the preservation of the biotite to be much better, with some flakes free of significant proportion of vermiculite or any other alteration product. In this area, the pyroclastic material was most probably transported by air, which would favour the measurement of the age of deposition. However, at present most of the outcrop has disappeared.

In Possagno, 7 probable bentonitic layers were collected from between volcano-sedimentary layers B1 and B18 (Fig. 4), spanning a time interval of less than 0.4 Ma. Each horizon contained euhedral biotite flakes (Table 1), as well as a non-magnetic, hydrochloric acid-insoluble sandy fraction of quartz and feldspar; the accessory minerals zircon and apatite were also present in all samples and were separated by heavy liquids and electromagnetic separator. Most of these layers have a constant thickness of between 2 and 5 cm; however, a few layers (B10, about 5 cm thick and biotite-rich) disappear laterally. The spectrum of minerals observed is typically volcanic and indicate that the layers found in the Marna di Possagno represent true bentonites, i.e. volcanic ashes deposited in a marine basin after aerial transport. The abundance and size of pyroclastic particles suggest a proximal volcanic source.

4.3. Preliminary study of the geochronometers

X-ray diffraction patterns undertaken in Paris indicate that idiomorphic "biotite flakes" from the Priabona area are actually vermiculite and chlorite with only a few per cent of micaceous sheets; the "biotite" flakes were found to have a K_2O content of 0.65%; they are unreliable geochronometers. In contrast, idiomorphic apatite and zircon crystals are perfectly transparent with well preserved crystal faces.

In Possagno, the feldspar was sanidine; however, after separation and ultra-sonic cleaning, crystals were found to be mostly non-idiomorphic, white and never transparent. Accordingly, in agreement with Baadsgaard and Lerbekmo [14], this feldspar was not considered to be a reliable geochronometer. The biotite fractions commonly show, for the bulk separates, the presence of between a few percent to more than 10% of a chlorite/vermiculite phase, indicating an alteration process of the volcanic material after eruption. However, the selected biotite concentrate from layer B9 was pure 10 Aå phase.

The quality of zircon and apatite crystals from Possagno was studied using cathodoluminescence (CL) observation in Paris (by GSO) and more

TABLE 1

Pyroclastic minerals from some volcano-sedimentary layers from early Late Eocene from Possagno and Priabona [a]

Layer	Level	Sand + silt	Biotite	Feldspar	Quartz	Zircon	Apatite
PosB1	0 m	75	0.8		present	present	present
PosB2	7 m	18	0.1	present	present		
PosB3	10 m	27	2.1				
PosB4	16.5 m	63	8		present		
PosB6	29.5 m	16	1		present		
PosB9	58.5 m	> 500	> 75	200	200	0.15	0.9
PosB10	68.5 m	400	190	abundant	abundant	0.07	0.9
Priabona	basal	≈15	up to 10	0	7	[b]	0.08

[a] All contents, in ‰ of the whole sediment, are approximations; unfilled columns indicate lack of analysis.

[b] Zircon content in Priabona was estimated to about 250 crystals per kg.

details were obtained in Berne (by VB). Investigation under CL is a powerful method for studying the growth history of minerals (e.g. [30] and references therein). This method assists interpretation of U–Pb ages because it seems that, for example, U, Th and Pb relative distribution correlates with the CL pattern in zircons [31], the luminescing regions being generally correlated with regions of higher U abundance [32].

CL microphotographs show fine oscillatory zoning in zircons from sample B9. This zonation is not apparent in transmitted, polarized, or reflected light under the petrographic microscope. No evidence of an inherited core was observed in the 10 studied grains (Berne) nor in Paris. The zircons are thus formed in situ in a single process and the zonation may be due to the crystallization process itself, as noted from carbonate crystals.

The CL spectra (Fig. 6) display two lines from dysprosium (Dy^{3+}) at 480 and 580 nm, and most likely also a third peak at 660 nm [30, 33, 34]. These lines are superimposed on a broad-band luminescence, which is considered by Mariano [in 30] as an intrinsic CL, attributed by Haberlandt [in 33] to uranium and by Marfunin [34] to radiation centres. A band at approximatively 390 nm is tentatively attributed to Eu^{2+}, although Mariano [in 30] points out that this "peak wavelength may

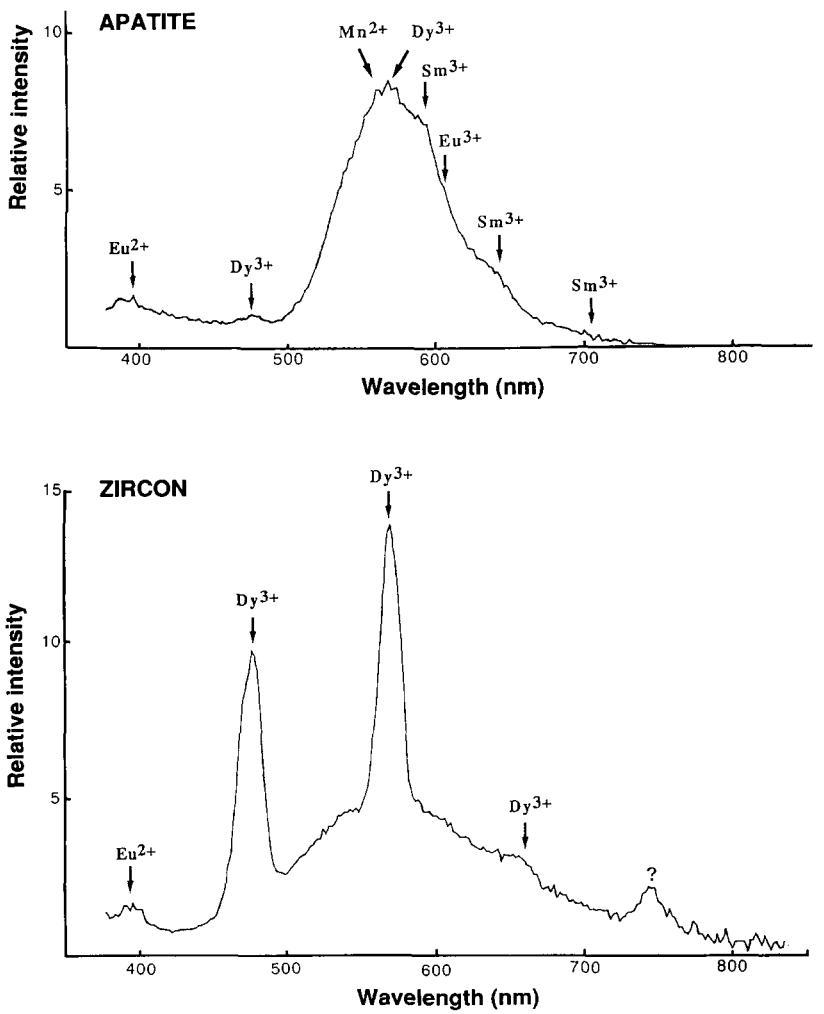

Fig. 6. Spectra of CL colours obtained from pyroclastic apatite (top) and zircon (bottom) single crystals (sample Pos B9). These spectra are corrected for instrumental response.

vary from about 410 nm to 450 nm depending on variations in the crystal field". An unidentified peak is observed at 740 nm.

Under CL, the apatite crystals show a uniform intensity distribution and no zonation has been observed. All of the 200 apatite grains show a yellow-green CL. The separate is homogeneous and no evidence for several populations of apatite was observed. The luminescence spectrum (Fig. 6) shows a broad-band emission around 570 nm,

TABLE 3

Fission track data measured for Priabonian samples

Sample and locality	Mineral and no. crystals	Spontaneous ρ_s (N_s)	Induced ρ_i (N_i)	$P\chi^2$ (%)	Reactor and glass	Dosimeter ρ_d (N_d)	Fission track age Ma ($\pm 1\sigma$)	Apatite mean track length (μm)	Length standard deviation (μm)
B-26	zircon	9.24	9.29	20	HERALD	0.665	37.2 ± 1.3		
(Odin)	20	(3515)	(3536)		CN1	(4700)			
	apatite	0.285	1.739	80	HERALD	1.295	35.9 ± 2.1	14.48 ± 0.11	0.84
	20	(395)	(2407)		SRM612	(5000)		(n = 57)	
POS B-9	zircon	7.56	7.52	65	PLUTO	0.611	34.5 ± 1.2		
(Odin)	12	(2151)	(2141)		CN1	(3880)			
	apatite	0.351	1.71	95	HIFAR	1.04	37.8 ± 1.6	13.92 ± 0.16	1.11
	16	(754)	(3676)		CN5	(7165)		(n = 51)	
POS/86	zircon	7.00	6.80	75	PLUTO	0.611	35.4 ± 1.5		
(Fischer)	12	(1367)	(1327)		CN1	(3880)			
B-1	zircon	7.91	7.52	75	PLUTO	0.611	36.2 ± 1.3		
(Barbin)	12	(1965)	(1867)		CN1	(3880)			
	apatite	0.217	2.21	90	PLUTO	2.265	38.6 ± 2.3	14.39 ± 0.14	1.14
	18	(324)	(3302)		SRM612	(15511)		(n = 70)	
Z-208	zircon	7.85	7.55	5	PLUTO	0.611	36.1 ± 2.1		
(Barbin)	7	(1412)	(1358)		CN1	(3880)			
	apatite	0.274	2.89	50	PLUTO	2.243	36.9 ± 2.1	14.16 ± 0.15	1.04
	15	(340)	(3588)		SRM612	(15511)		(n = 50)	
Zircon age standards									
Fish	zircon	5.535	8.395	55	HERALD	0.749	27.8 ± 1.1		
Canyon	20	(2778)	(4213)		CN1	(4700)			
Tuff									
	zircon	6.31	8.127	45	PLUTO	0.611	26.8 ± 0.8		
	14	(2910)	(2910)		CN1	(3880)			
Buluk	zircon	1.149	2.869	65	HERALD	0.742	16.8 ± 0.7		
Member	20	(1433)	(3579)		CN1	(4700)			
Tuff									
Apatite age standards									
Durango	apatite	0.178	2.355	60	PLUTO	2.265	30.0 ± 1.9		
	13	(255)	(3373)		SRM612	(15511)			
Fish	apatite	0.195	2.644	95	PLUTO	2.267	28.9 ± 1.8		
Canyon	20	(280)	(3790)		SRM612	(15511)			
Tuff									

Notes

Track densities (ρ) are as measured and are ($\times 10^6$ tr cm^{-2}); numbers of tracks counted (N) shown in brackets.

Analyses by external detector method using 0.5 for the $4\pi/2\pi$ geometry correction factor.

Ages calculated using zircon $\zeta_{CN1} = 113 \pm 3$; apatite (HERALD) $\zeta 612 = 339 \pm 5$; apatite (PLUTO) $\zeta 612 = 348 \pm 9$; apatite (HIFAR) $\zeta_{CN5} = 355 \pm 5$.

$P\chi^2$ is probability for obtaining χ^2 value for v degrees of freedom, where v = no. crystals − 1.

Independent ages of Fish Canyon Tuff = 27.8 ± 0.1 Ma [38]; Durango = 31.4 Ma; Buluk Member Tuff = 16.4 ± 0.2 Ma [38].

TABLE 2

K–Ar radiometric results obtained in Gif-sur-Yvette from the biotite from layer B9, mid Late Eocene from Possagno

K content (%)	% radiogenic	Ar (nl/g)	Apparent age Ma $\pm 2\sigma$
6.13 ± 0.11 [a]	82.8	8.40 ± 0.08	34.7 ± 0.7
6.22 ± 0.11 [b]	86.7	8.54 ± 0.08	35.3 ± 0.7

[a] Atomic absorption.
[b] Flame photometry (the mean value was used for apparent age calculations).

which is mainly attributed to the presence of Mn^{2+} [35]. Dy^{3+} and Sm^{3+} peaks are also present but masked by the broad band Mn^{2+} emission [35]. A small band occurring at 390 nm is tentatively assigned to Eu^{2+}.

In summary, the bentonitic nature of the biotite-rich layers is well documented in Possagno, as in Massignano. In Priabona, a secondary deposition is suspected: the mud flow is thicker and the biotite is entirely altered probably in connection with this redeposition process. The homogeneity of the separated geochronometers seems good enough to suggest that they come from a single volcanic event. The preservation of the selected geochronometers also appears good.

5. Radiometric results

The K–Ar method was applied as a matter of reference for comparison with the following two dating methods. The purest biotite sample was collected from the richest layer of the section in Possagno.

The analytical results are shown in Table 2 with 2σ errors estimated according to the usual long-term reproducibility of measurements in the laboratory. The weighted mean age of 35.0 ± 0.5 (2σ) Ma for this mid-Priabonian sample compares well with the age of the Priabonian stage, located between 37–38 and 34 Ma, as supported by the present first author [1, 3, 4, 5, 7, 36].

Fission track dating results are shown in Table 3. The interpretation of the apatite apparent ages was considered using confined track length measurements made on the four apatite separates (Fig. 7). They each show tight volcanic-type length distributions of long tracks, with mean values around 14 μm and standard deviations around 1 μm [37]. Such values are also found for Fish Canyon Tuff and Durango apatite age standards [38] and can be taken as evidence that these samples cooled rapidly and have not been subjected to partial track loss by low-temperature reheating. These measured apatite ages can thus be interpreted as formation ages.

Zircon ages for the 3 samples from layer B9 in Possagno (Pos B-9, Z 208, Pos/86, see Table 3) have a weighted mean of 35.1 ± 1.8 (2σ) Ma, a value slightly lower than, but overlapping with the weighted mean apatite age of 37.5 ± 2.6 (2σ) Ma for the same horizon (Pos B9, Z 208). Since this is the reverse of the stabilities of the two minerals for track annealing (apatite anneals between 60 and 110°C and zircon ~ 230°C over geological time), this difference in age is probably a random variation within track counting statistics, as reflected by the errors on individual measurements. The similarity within analytical error of apatite and zircon implies that the sample has cooled rapidly and has not been subjected to reheating above about 50°C since formation/deposition. A similar coincidence can be seen between apatite and zircon ages for sample B1 from Possagno and sample B26 from Priabona. We have calculated composite (zircon + apatite) weighted mean ages for each dated layer: 36.8 ± 2.2 (2σ) Ma in Bucco della Rana; 36.8 ± 2.2 (2σ) Ma for sample B1;

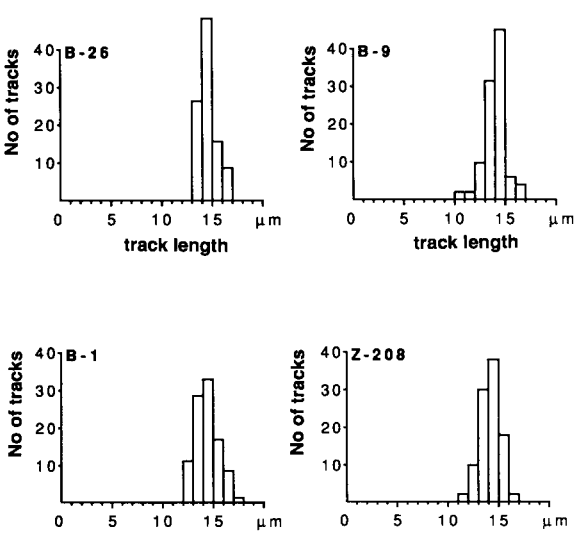

Fig. 7. Horizontal confined track length measurements in the apatite samples. The narrow distribution culminating at 13–15 μm indicates absence of annealing.

TABLE 4

U–Pb radiometric results obtained in Edmonton from zircons separated from the biotite-rich layer B9 (mid Late Eocene from Possagno)

Sample	$^{206}Pb/^{204}Pb$ [a]	^{238}U (ppm)	^{206}Pb (ppm)	Common Pb (ppm) [b]	$^{206}Pb/^{238}U$	$^{207}Pb/^{235}U$
> 99 μm						
A	3968 ± 80	583.5	4.468	0.036	0.00885	0.0785
B	3704 ± 10	588.7	4.618	0.035	0.00906	0.0819
C	3303 ± 9	590.6	4.642	0.049	0.00908	0.0846
− 99 + 74 μm						
A	2967 ± 22	620.0	4.696	0.059	0.00875	0.0782
B	3049 ± 15	617.8	4.351	0.037	0.00814	0.0680
C	2825 ± 18	618.3	4.591	0.052	0.00858	0.0757
HF	5348 ± 40	610.3	4.911	0.035	0.00930	0.0847
− 74 + 58 μm						
A	4310 ± 29	647.7	4.965	0.042	0.00886	0.0781
B	4878 ± 48	649.9	5.121	0.033	0.00910	0.0807
C	5714 ± 33	647.1	4.980	0.032	0.00889	0.0782
< 58 μm						
A	4831 ± 43	681.1	4.877	0.038	0.00880	0.0757
B	6289 ± 63	686.7	5.556	0.030	0.00935	0.0833
C	5236 ± 27	681.8	5.247	0.025	0.00889	0.0774
HF	2433 ± 12	686.1	4.913	0.084	0.00951	0.0841

[a] Pb isotope ratios normalised to NBS sample SRM 981 lead values.
[b] Common Pb composition used: 204 = 1; 206 = 18.657; 207 = 15.626; 208 = 38.576.

and 35.8 ± 1.4 (2σ) Ma for the biotite-rich layer B9. The latter weighted mean ages compare well with the K–Ar biotite age of 35.0 ± 0.5 Ma obtained from sample B9.

In summary, the application of fission track dating appears fruitful for obtaining moderately precise (±4 to 5%, 2σ errors) ages where no K-bearing geochronometers are present. More-

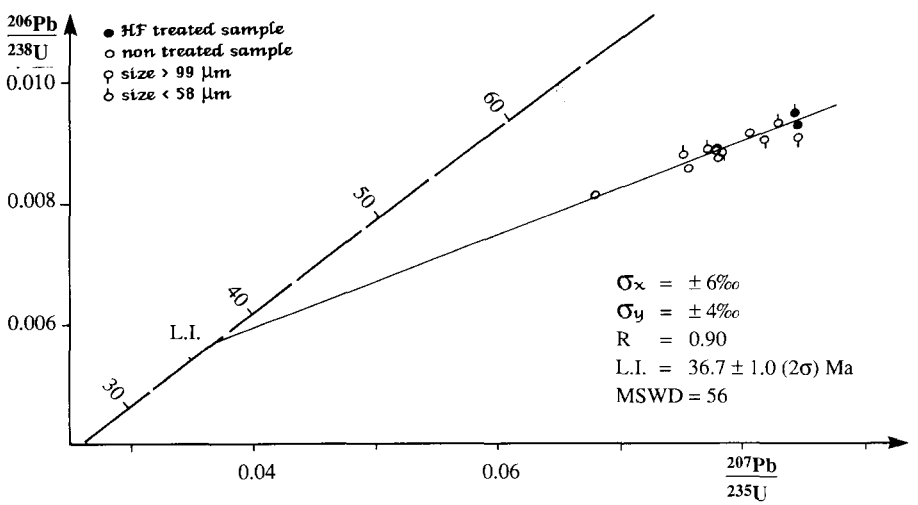

Fig. 8. Concordia diagram showing the results obtained from zircons separated from layer B9 in Possagno.The fourteen analytical points roughly spread along a discordia line. Black dots = HF treated samples; open dots non-treated samples.

over, this dating method permits identification of the quiet thermodynamic history of the dated outcrop.

U–Pb dating of young zircons is not commonly undertaken; however, recent research on Phanerozoic pyroclastic zircons, including mid-Tertiary zircons [19, 39] has shown the feasibility of such analyses. In the present study, fourteen fractions of zircon were analysed, the analytical results being summarized in Table 4, and represented in a concordia diagram (Fig. 8). The following points should be emphasized.

(1) All analytical results are located far from the concordia–discordia lower intercept (they are very discordant on the concordia plot), and 13 of the 14 data draw a comparatively short elongated cloud of points. Accordingly, the quoted intercept will not be precisely defined for these very discordant zircons.

(2) For each of the 4 size fractions, 3 different aliquots were analysed: A, B, C. The results indicate a fairly constant amount of uranium within each size fraction with more U in the smaller size fractions (column ^{238}U in Table 4); however, there are surprisingly wide variations in the amounts of radiogenic ^{206}Pb within each size fraction. Such variations were not obtained in previous analyses of pyroclastic zircons [19, 39]; moreover, the different size fractions do not show a decrease of the amount of contaminant common lead with decrease of the size-fraction as is usually observed.

(3) In an attempt to obtain data closer to the lower intercept by the removal of contaminant common lead, 2 size fractions were treated with HF (samples HF in Table 4). However, in contrast to frequent observations [19], in these samples the amount of common lead was unaffected by the HF treatment; in the smaller size fraction the amount of common lead was found to be even greater after treatment. Thus in this study at least, the HF treated samples result in data farther from the intercept than the untreated samples. One possibility may be that contamination was introduced during the HF treatment.

(4) The proportion of radiogenic lead is very high in these zircons ($^{206}Pb/^{204}Pb$ above 2000 and up to 6300); therefore, the assumed common lead initial isotopic composition (Stacey-Kramers 35 Ma old lead) is not critical to the results.

(5) Calculation of the age corresponding to the lower intercept was made using uncorrelated ($R = 0$) and correlated ($R = 0.90$) regression analyses. These two calculations give results that are the same within error, i.e.: $37.3 + 3.0/-3.2$ (2σ) Ma and 36.7 ± 1.0 (2σ) Ma, respectively; the correlated regression is the preferred treatment. With this treatment, the upper intercept discordia–concordia corresponds to an age of 1513 ± 48 Ma, an age with no geological meaning.

(6) Replicate determinations on finely ground Tertiary zircon powder in Edmonton give a current reproducibility of: $\pm 0.4\%$ (2σ) on uranium data; $\pm 0.5\%$ (2σ) on ^{206}Pb data; $\pm 0.8\%$ (2σ) on ^{207}Pb data.The total lead blank for a zircon determination is currently 0.32 ng and that for uranium is 0.8 pg. Because the scatter of data points on the concordia plot is outside the limits of analytical reproducibility, with a MSWD = 56, sample heterogeneity or analytical errors are probably present. This means that the extrapolated intercept ages are to be considered approximations to the real ages and the statistical errors associated with the intercepts have no strict time meaning (F. Oberli pers. commun., 1991).

(7) The apparent zircon U–Pb age of 36.7 ± 1.0 (2σ) Ma is consistent with the fission track zircon and apatite mean age within error limits, but is slightly older than the more precise and more reliable K–Ar biotite age of 35.0 ± 0.5 Ma.

6. Discussion

6.1. K–Ar results and comparison with previous studies

The stratigraphic location of sample B26 from Priabona is well established near the base of the Priabonian stage. In Possagno, sample B1 is located within a normal palaeomagnetic episode which is tentatively correlated here to the 16 N1 reversal of the section in Massignano; B9 is only 0.1 to 0.3 Ma younger. The two levels are in the calcareous nannofossil biozone NP 19–20 and the planktonic foraminiferal zone P16 of the oceanic zonations. They are, therefore, assumed to be slightly younger by less than 2 Ma, possibly 1 Ma, than the sample dated in the Priabona area. In Massignano (Apennines), 3 biotite-bearing layers corresponding to the same position within magnetostratigraphic episode 16 N1 and slightly above

were identified [27, 40]; a precise contemporaneity and common origin with the events in Possagno is not yet proved.

Fischer et al. [41] presented results of U–Pb dating of zircons from bentonite B 9 from Possagno. They concluded a "maximum age of 35.4 Ma corroborated by a mean K–Ar age of 34.2 Ma for cogenetic biotite". Taking into account the error margins, there is reasonably good agreement between our K–Ar age and the study in Zürich (F. Oberli, pers. commun., 1991).

Radiometric dates were also obtained from time equivalent biotite-rich layers collected from the Apennines [7]. In Massignano, biotite from meter level 7.20 was considered one of the most reliable geochronometers of the series: 3 K–Ar dates with a mean of 35.3 ± 0.5 Ma and 2 Rb–Sr dates with a mean of 36.2 ± 0.4 Ma were measured. In the Gubbio area, a time equivalent biotite-rich layer was dated at 35.4 ± 0.2 Ma with the Rb–Sr method and a slightly older layer (about 1 Ma older according to sediment thickness interpolation) was dated at 36.4 Ma (mean of 3 K–Ar dates).

Therefore, the present K–Ar result (35.0 Ma) from the Possagno section compares favourably with previous dates from the Apennines. Taken together, there is no doubt that the age of eruption of the volcanics and subsequent deposition of the tephra from the mid Priabonian in Italy is between 35 and 36 Ma.

6.2. *Comparison of FT and K–Ar results*

In the fission track results presented above, the errors representing analytical uncertainties in Table 3 are generally higher for apatite (± 3.2 to 4.2 Ma at 2σ) than for zircon (± 2.4 to 3.0 at 2σ, with an unusually high ± 4.2 Ma for Z 208). These uncertainties result from more tracks being counted in zircon analyses than in apatite determinations, reflecting the higher uranium contents of zircon. However, as far as reproducibility of results is concerned, the high consistency of the various data suggest the calculated 2σ errors may be unduly pessimistic. Combination of multiple individual ages measured for level B9 reduces the 2σ error to ± 1.4 Ma, a far more acceptable value for time-scale calibration. This value further represents a realistic assessment of analytical uncertainty since it results from dating analyses on two different minerals from three different samples collected from the same stratigraphic level by three different geologists who independently separated the dated minerals.

Note that Pos B9 and B1 included two apatite crystals of rounded form with significantly older apparent ages (around 70 Ma). These crystals may represent "inherited" crystals and thus have been excluded from the ages for samples presented in Table 3. We believe this approach to be acceptable in respect of the nature of the material dated, volcanic ash erupted during explosive acid volcanism. The occurrence of material from different sources and, therefore, of different ages, is a constant problem in such studies. Determination of single-crystal ages using the fission track external detector method provides a direct mean of identifying such heterogeneity. The detailed cathodoluminescence study has not shown such heterogeneity in apatite nor in zircon rough separates obtained in Berne or Paris; the significantly older ages might therefore be due to subsequent sample pollution.

In addition to the concordancy of zircon and apatite FT ages, the consistency of ages measured for different samples of the same horizon and the preservation of apatite undisturbed volcanic-type confined track lengths, the excellent agreement between the fission track ages and ages obtained from coeval K-rich biotites provides a further positive control of the reliability of the fission track dating results.

6.3. *Relation of U–Pb results to the other ages*

U–Pb radiometric dating of young material is problematic [19, 39]. In the present study, we have investigated whether U–Pb dating of 35 Ma old zircons from bentonites can usefully contribute to the calibration of the time scale. Unfortunately, the dated zircons were very 'discordant' on the concordia plot. The usual interpretation of a concordia plot drawn from U–Pb analytical results obtained from pyroclastic zircons, considers that the lower intersection of the discordia line (where data points group) with the concordia (the curve where $^{238}U-^{206}Pb$ and $^{235}U-^{207}Pb$ apparent ages are similar) represents the time of eruption of the zircons. In these circumstances, these zircons are interpreted as variably contaminated with pre-ex-

isting radiogenic lead; this may result from a physical mixing process involving inherited and syn-volcanic crystals or portions of zoned crystals. This has been called type 2 discordancy [14]. The type 1 discordancy refers to a lead loss following the dated geological event and has been found to occur in Silurian zircons from Gotland [42] which show intersection ages younger than the K–Ar ages of cogenetic biotites [43]. In the present situation, however, the difference of the apparent ages obtained (according to the process of calculation using uncorrelated and correlated regressions), would seem to indicate the discordia to result from something more complex than a lead loss or simple mixing pattern. Detailed analysis of the data along the discordia line reveals that the 3 points representative of the larger zircon crystals (> 99 μm) are spread along and below the line, whilst the 4 points representative of the smaller zircons (< 58 μm) are similarly spread above the line.

The zircons from Possagno can be considered to be closed mineral systems since their time of deposition because weathering, heating, deep burial, tectonism or significant metamictization have not affected them, as observed in the field and confirmed by the fission track study. Accordingly, the scatter of points along the discordia line may be explained by the acquisition by the zircons of older contaminants, most probably older zircons of a relatively definite age. If the older contaminant zircons were of variable age, a scattering of measured bulk zircon data points such as observed in this data set can occur. Such contamination may relate to the presence of a few apparently older and inherited apatite crystals, some of them identified during fission track analysis; however, the detailed cathodoluminescence observation does not confirm this point as discussed above. According to F. Oberli (pers. commun., 1991), the discordancy and unusual behaviour of U–Pb results are more probably related to the presence of inclusions (with various initial Pb isotopic compositions) within zircon crystals as shown by his work in progress using U–Pb ion microprobe analysis.

Concerning the geological interpretation of the calculated age, this contamination mainly influences the scatter of points along and on both sides of the discordia line increasing the analytical error. The calculated $\pm$ on a U–Pb age is significantly smaller than uncertainties calculated using the fission track approach. Because the calculated U–Pb age is consistent with that obtained using K–Ar dating on the same layer, and those obtained form nearly coeval layers in the Apennines, it is apparent that the cause of the "unusual behaviour" observed does not heavily bias the geological age.

In summary, the U–Pb dating of the Late Eocene zircons has not been unsuccessful, their discordant nature and unusual behaviour regarding HF treatment and heterogeneous composition of each size fraction means the results should be supplemented with microanalyses. However, the feasibility of dating such young zircons is confirmed.

6.4. Age and duration of the Priabonian stage

The Priabonian stage is located in one of two different portions of the numerical time scale: either between 40 and 36.5–37 Ma (i.e. by Palmer [2]), or between 37–38 and 34 Ma (i.e. by Odin and coll. [1, 4, 36]), depending on the authors. An important point is that Palmer's time scale is the result of a continuous, long-term, extrapolation. Thus, if it is shown that a given point of such a scale is not correct, the whole larger extrapolated portion containing this point will also be incorrect. Use of such a scale could lead to the incorrect stratigraphical allocation of all rocks, despite being correctly dated radiometrically, throughout a substantial portion of the stratigraphic sequence.

Concerning the duration of the stage, the extrapolation principle using relative thicknesses of oceanic sea-floor anomalies favoured by Palmer can be considered a generally acceptable approach. However, the problem does not lie there because the two alternative scales agree for the duration of the Priabonian (3 to 4 million years long).

Following this argument, convincing evidence for the age of one point within the stage would provide sufficient means to test the validity of one or other proposal. Such convincing evidence is difficult to obtain for time-scale calibration purposes due to the variety of possible biases shown by individual apparent ages. Our long-term objective in this research has been to gather ages from different depositional basins, from different geo-

chronometers and using different dating methods implemented in different laboratories. Only by such a route can a consensus agreement be reached.

Additional recently published ages obtained from pyroclastic geochronometers can also be cited. Nagymarosy et al. [44] reported biotite ages between 33 and 34 Ma just above the Eocene–Oligocene boundary, i.e. the younger limit of the Priabonian stage (K–Ar conventional technique: 32.2 ± 0.9 Ma; $^{40}Ar-^{39}Ar$ technique: 33.7 ± 1.0 Ma for total fusion and 34.3 ± 1.3 Ma for plateau age); Glass et al. [45] concluded an age of 34.4 ± 0.6 Ma for the same boundary following microtektite laser fusion $^{40}Ar-^{39}Ar$ measurements. In the Apennines, an age of 33.7 ± 0.5 Ma [7, 26] is concluded from a series of radiometric dates measured from biotite separates from both above and below the same boundary. This conclusion combines ages derived from both the Rb–Sr and K–Ar methods, with different K–Ar analytical techniques implemented in Hannover (conventional K–Ar technique) and Leeds ($^{40}Ar-^{39}Ar$ technique). The present study indicates perfect agreement between previous K–Ar biotite ages obtained in the Apennines (Priabonian between about 37 and 33.7 Ma) and the new result obtained in another laboratory from a biotite (mid-Priabonian at 35 Ma) from the Southern Alps. All of these results support the young ages for the Priabonian portion of the stratigraphic sequence. They also confirm the ages proposed from a combination of consistent radiometric ages obtained in 1978 [1] from dominantly glaucony analyses and a few volcanic geochronometers. Such new data validates the inclusion of the glaucony dates and argues strongly that the ages were reliable.

This is also of great consequence for the Decade of North American Geology conventional scale [2], widely quoted in the literature, and shown here to be incorrect with a local deviation of about 3 Ma for the Priabonian, a bias of about 10% of the actual age. Two of the six tie points selected for calculating this extrapolated scale between 0 and 84 Ma [46] are at 32.4 and 34.6 Ma. These ages were considered to correspond to levels well inside the Oligocene, but as is shown in the present study, they correspond to the basal boundary of the Oligocene. Thus these tie points of extrapolation are not only doubtful [3, 5] but incorrect. Because the scale is now shown to be incorrect for the 34 Ma region, and the next tie points of the extrapolated scale are at about 9 Ma and 50 Ma, the implication is that the whole portion between 9 and 50 Ma is also incorrect. Large portions of the Palaeogene and Neogene Decade of North American Geology time scale should therefore be revised to conform these new radiometric dates. Material for such revision was gathered in the Apennines, is presented here for the Late Eocene and will be presented in the near future for the Neogene. Most of this work is undertaken under the aegis of the Subcommission on Geochronology and other bodies of IUGS which facilitate the interdisciplinary, multi-method, multi-laboratory approach necessary for time-scale calibration purposes. This diversified approach is currently the single way to reach consensus in the field of time-scale calibration.

Acknowledgements

Permission for working in the quarry of Antonio Cunial in Possagno was greatly appreciated. Don Elio (Nizzero) welcomed the authors in Priabona during the last 5 years, a great help which is deeply acknowledged. In addition to some of us (VB, BG and GSO), sample collection was made with the help of Professors R. Herb and F. Proto Decima (once) and M. Zelvelder (twice). This work benefited from the biostratigraphical discussion with F. Proto Decima and M. Toumarkine. Y. Cornette helped us to measure K and Ar at Gif. M.G. Bonhomme and M. Zelvelder prepared and dated the clay from Bucco della Rana. This work also benefited from the geochronological discussion with F. Oberli. J.C. Hunziker and two anonymous reviewers contributed to improvement of the manuscript. All are gratefully thanked. Grants for sample collections were generously provided by the French National committee of IGCP (UNESCO–IUGS) in 1987 and 1989. Fission track dating in London was supported by NERC Grant GR3/7068 and a BP research award.

References

1 G.S. Odin, D. Curry and J.C. Hunziker, Radiometric dates from NW European glauconies and the Palaeogene time scale, J. Geol. Soc. London 135, 481–497, 1978.

2 A.R. Palmer, Geologic time scale, Geology 11, 503–504, 1983.
3 G.S. Odin, The Palaeogene time scale, geochronological discussion of an interpolated version, Bull. Liais. Inform., IGCP Project 196, offset, 6, 11–26, 1986.
4 G.S. Odin, Ages radiométriques récemment obtenus dans la séquence stratigraphique paléogène, Bull. Soc. géol. Fr. 8, 145–152, 1989.
5 G.S. Odin and D. Curry, D., The Palaeogene time scale: radiometric dating versus magnetostratigraphic approach, J. Geol Soc. London 142, 1179–1188, 1985.
6 A. Montanari, R. Drake, D.M. Bice, W. Alvarez, et al., Radiometric time scale for the upper Eocene and Oligocene based on K–Ar and Rb–Sr dating of volcanic biotites from the pelagic sequence of Gubbio, Italy, Geology 13, 596–599, 1985.
7 G.S. Odin, A. Montanari, A.L. Deino, R. Drake, P. Guise, H. Kreuzer and D.C. Rex, Reliability of volcano-sedimentary biotite ages across the Eocene/Oligocene boundary, Chem. Geol. (Isot. Geosci. Sect.) 86, 203–224, 1991.
8 V. Barbin, Le Priabonien dans sa région type (Vicentin, Italie); stratigraphie, micropaléontologie, Mém. Sci. Terre Univ. P. and M. Curie, Paris, 86–29, 281 pp., 1986.
9 H.M. Bolli, ed., Monografia micropaleontologia sul Paleocene e l'Eocene di Possagno, provincia di Trevisio, Italia, Schweiz, Paläontol. Abh., Basel, 97, 220 pp., 1969.
10 B. Galbrun, J. Gabilly and L. Rasplus, Magnetostratigraphy of the Toarcian stratotype sections at Thouars and Airvault (Deux-Sèvres, France), Earth Planet. Sci. Lett. 87, 453–462, 1988.
11 K. Ramseyer, J. Fischer, A. Matter, P. Eberhardt and J. Geiss, A cathodoluminescence microscope for low intensity luminescence, J. Sediment. Petrol. 59, 619–622, 1989.
12 G.S. Odin and 35 collaborators, Interlaboratory standards for dating purposes, in: Numerical Dating in Stratigraphy, G.S. Odin, ed., pp. 123–150, John Wiley, Chichester, 1982.
13 P.-Y. Gillot and Y. Cornette, The Cassignol technique for potassium–argon dating, precision and accuracy: examples from the Late Pleistocene to Recent volcanics from southern Italy, in: Calibration of the Phanerozoic Time Scale, G.S. Odin, ed., Spec. Issue, Chem. Geol. (Isot. Geosci. Sect.) 59, 205–222, 1986.
14 H. Baadsgaard and J.F. Lerbekmo, The dating of bentonite beds, in: Numerical Dating in Stratigraphy, G.S. Odin, ed., pp. 423–440, John Wiley, Chichester, 1982.
15 A.J.W. Gleadow, Fission track dating methods: what are the real alternatives? Nuclear Tracks 5, 3–14, 1981.
16 A.J. Hurford and P.F. Green, The zeta age calibration of fission track dating. Chem. Geol. (Isot. Geosci. Sect.) 1, 285–317, 1983.
17 R.F. Galbraith, On statistical models for fission track counts, Math. Geol. 13, 471–488, 1981.
18 P.F. Green, A new look at statistics in fission track dating, Nuclear Tracks 5, 77–86, 1981.
19 H. Baadsgaard, J.F. Lerbekmo and I. McDougall, A radiometric age for the Cretaceous–Tertiary boundary based upon K–Ar, Rb–Sr, and U–Pb ages of bentonites from Alberta, Saskatchewan and Montana, Can. J. Earth Sci. 25, 1088–1097, 1988.
20 E. Munier-Chalmas and A. De Lapparent, Note sur la nomenclature des terrains sédimentaires, Bull. Soc. géol. Fr. 21, 438–488, 1893.
21 J. Hardenbol, The Priabonian type section, a preliminary note, Colloque Eocène, Paris, Mém. B.R.G.M., Orléans 58, 629–636, 1969.
22 M.B. Cita, Le Paléogène et l'Eocène de l'Italie du Nord, Colloque Eocène Paris, Mém. B.R.G.M., Orléans 69, 417–428, 1969.
23 V. Barbin, The Eocene–Oligocene transition in shallow water environment: the Priabonian stage type area (Northern Italy), Int. Subcomm. Paleogr. Stratigr., Eocene/Oligocene Meeting, Ancona, Spec. Publ., 163–171, 1988.
24 C. Gruas-Cavagnetto and V. Barbin, Les Dinoflagellés du Priabonien stratotypique (Vicentin, Italie); mise en évidence du passage Eocene–Oligocene, Rev. Paléobiol., Genève 7, 163–198, 1988.
25 C. Gruas-Cavagnetto and V. Barbin, La palynoflore (spores–pollens) du Priabonien stratotypique (Vicentin, Italie), Rev. Paléobiol., Genève 8, 95–120, 1989.
26 G.S. Odin and A. Montanari, Age radiométrique et stratotype de la limite Eocène–Oligocène, C.R. Acad. Sci. Paris 309, 1935–1945, 1989.
27 G.S. Odin, S. Clauser and M. Renard, Sedimentological and geochemical data on the Eocene/Oligocene boundary at Massignano, (Apennines, Italy), Int. Subcom. Paleogr. Stratigr., Eocene/Oligocene Meeting, Ancona, Spec. Publ., 175–186, 1988.
28 D.M. Bice and A. Montanari, Magnetic stratigraphy of the Massignano section across the Eocene–Oligocene boundary, Int. Subcomm. Paleogr. Stratigr., Eocene/ Oligocene Meeting, Ancona, Spec. Publ., 111–118, 1988.
29 V. Barbin and A. Keller Grünig, Benthic foraminiferal assemblage of Brendola (N. Italy), Mar. Micropal. 17, 3, 181–199.
30 D.J. Marshall, Cathodoluminescence of Geological Materials, 146 pp., Unwin Hyman, Boston, 1988.
31 B. Grauert and M.E. Wagner, Age of the granulite-facies metamorphism of the Wilmington complex, Delaware, Am. J. Sci. 275, 683–691, 1975
32 R.D. Vocke and G.N. Hanson, U–Pb zircon ages and petrogenetic implications for two basement units from Victoria valley, Antarctica, in: Antarctic Research Series, Washington, Am. Geophys. Union, 33, 247–255, 1981.
33 A.K. Trofimov, The luminescence spectrum of zircon, Geochemistry 11, 1102–1108, 1962.
34 A.S. Marfunin, Physics of Minerals and Inorganic Materials, 250 pp., Springer-Verlag, Berlin, 1979
35 P.L. Roeder, D. MacArthur, X.P. Ma, G.R. Palmer and A.N. Mariano, Cathodoluminescence and microprobe study of rare-earth elements in apatite, Am. Mineral. 72, 801–811, 1987.
36 G.S. Odin and C. Odin, Echelle numérique des temps géologiques, mise à jour 1990, Géochronique 35, 12–21, 1990.
37 A.J.W. Gleadow, I.R. Duddy, P.F. Green and J.F. Lovering, Confined fission track lengths in apatite: a diagnostic tool for thermal history analysis, Contrib. Mineral. Petrol. 94, 405–415, 1986.
38 A.J. Hurford, Standardization of fission track dating calibration: recommendation by the Fission Track Working

Group of the IUGS Subcommission on Geochronology, Chem. Geol. (Isot. Geosci. Sect.) 80, 171–178, 1990.

39 H. Baadsgaard and P.A. Cavell, U–Pb dating of Phanerozoic zircon, Bull. Liais. Inf. IGCP Proj. 196, offset, Paris 7, 49–53, 1988.

40 G. Parisi and R. Coccioni, Deep-water Foraminifera at the Eocene–Oligocene boundary in the Massignano section, Int. Subcomm. Paleogr. Stratigr., Eocene/Oligocene Meeting, Ancona, Spec. Publ., 97–109, 1988.

41 H. Fischer, F. Oberli and M. Meier, Zircon dating of Oligocene and Miocene bentonites by the U–Pb method, Abstracts, EUG V, Terra Abstr. 1, 419, 1989.

42 P.A. Cavell and H. Baadsgaard, U–Pb systematics of zircons from Silurian bentonites, Gotland, Sweden, Bull. Liais. Inf. IGCP Proj. 196, offset, Paris 6, 65–67, 1986.

43 G.S. Odin, J.C. Hunziker, L. Jeppsson and N. Spjeldnaes, Radiometric K–Ar ages of pyroclastic biotites deposited in the Wenlockian of Gotland (Sweden), Chem. Geol. (Isot. Geosci. Sect.) 59, 117–126, 1986.

44 A. Nagymarosy, Y. Takigami and K. Balogh, Stratigraphic position and the radiometric age of the Kiscellian stratotype, Hungary, Bull. Liais. Inform., IGCP Project 196, offset, 6, 29–32, 1986.

45 B.P. Glass, C.M. Hall and D. York, $^{40}Ar-^{39}Ar$ laser probe dating of North American tektite-fragments from Barbados and the age of the Eocene–Oligocene boundary, Chem. Geol. (Isot. Geosci. Sect.) 59, 181–186, 1986.

46 B. Berggren, D.V. Kent and J.J. Flynn, Paleogene geochronology and chronostratigraphy, Mem. Geol. Soc. London 10, 141–198, 1985.